

Perfect Cubic Aromatic Metallo-Borospherenes TM_8B_6 (TM = Ni, Pd, Pt) As Superatoms Matching the 18-Electron Rule

Mei-Zhen Ao,^{a,b} Yuan-Yuan Ma,^c Yue-Wen Mu,^{*a} and Si-Dian Li^{*a}

^aInstitute of Molecular Science, Shanxi University, Taiyuan 030006, China.

^bFenyang College of Shanxi Medical University, Fenyang 032200, China

^cShanxi Institute of Energy, Taiyuan 030006, China

*E-mail: ywmu@sxu.edu.cn and lisidian@sxu.edu.cn

Table of Contents

Figure S1. Low-lying isomers of Ni_8B_6 .

Figure S2. Low-lying isomers of Pd_8B_6 .

Figure S3. Low-lying isomers of Pt_8B_6 .

Figure S4. Low-lying isomers of $\text{Ni}_8\text{B}_6^{-1}$.

Figure S5. BOMD simulations of (a) $O_h \text{Ni}_6\text{B}_6$ (**1**), (b) $O_h \text{Pd}_6\text{B}_6$ (**2**), and (c) $O_h \text{Pt}_6\text{B}_6$ (**3**) at different temperatures.

Figure S6 The $1\text{S}^21\text{P}^61\text{D}^{10}$ 18-electron configurations of $O_h \text{Pd}_8\text{B}_6$ (**2**) and $O_h \text{Pt}_8\text{B}_6$ (**3**) and (b) AdNDP bonding patterns of $O_h \text{Pd}_8\text{B}_6$ (**2**) and $O_h \text{Pt}_8\text{B}_6$ (**3**).

Figure S7. Simulated IR, Raman and UV-vis spectra of (a) $O_h \text{Pd}_8\text{B}_6$ and (b) $O_h \text{Pt}_8\text{B}_6$.

Table S1. Optimized cartesian coordinates (x, y, z) of (a) $O_h \text{Ni}_6\text{B}_6$ (**1**), (b) $O_h \text{Pd}_6\text{B}_6$ (**2**), (c) $O_h \text{Pt}_6\text{B}_6$ (**3**), and (d) $O_h \text{Ni}_8\text{B}_6^{-1}$ (**1'**) at PBE0/6-311+G(d) level.

Figure S1. Low-lying isomers of Ni₈B₆ with its relative energies indicated in eV at PBE0 and TPSSh (parentheses) levels, respectively.

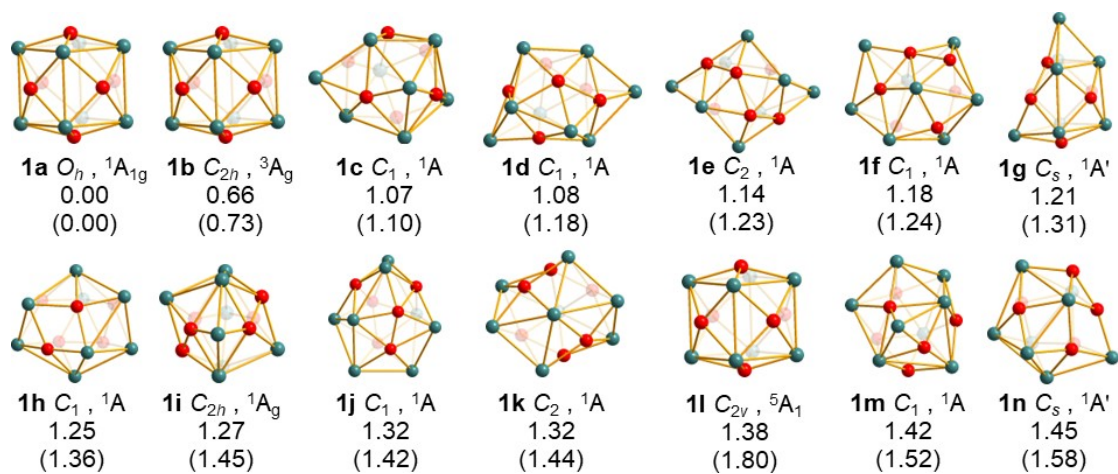


Figure S2. Low-lying isomers of Pd₈B₆ with its relative energies indicated in eV at PBE0 and TPSSh (parentheses) levels, respectively.

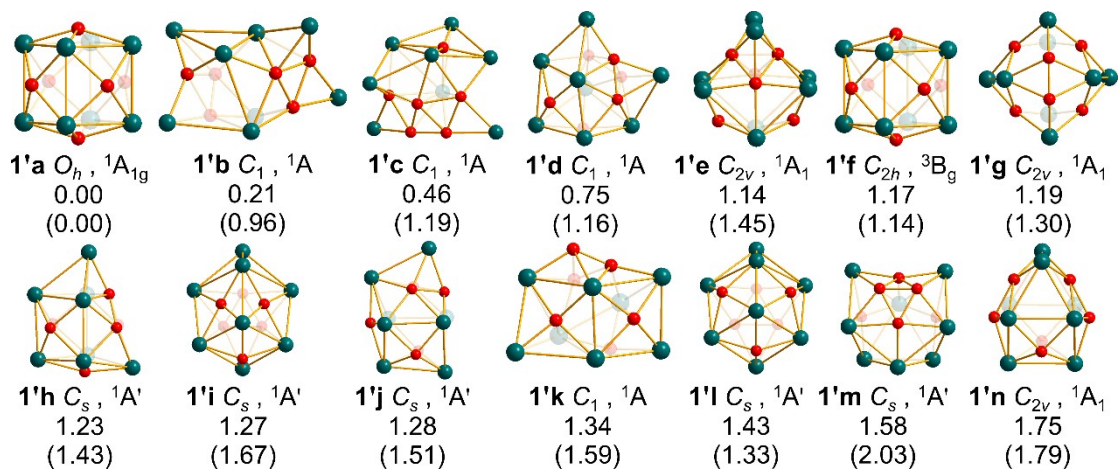


Figure S3. Low-lying isomers of Pt_8B_6 with its relative energies indicated in eV at PBE0 and TPSSh (parentheses) levels, respectively.

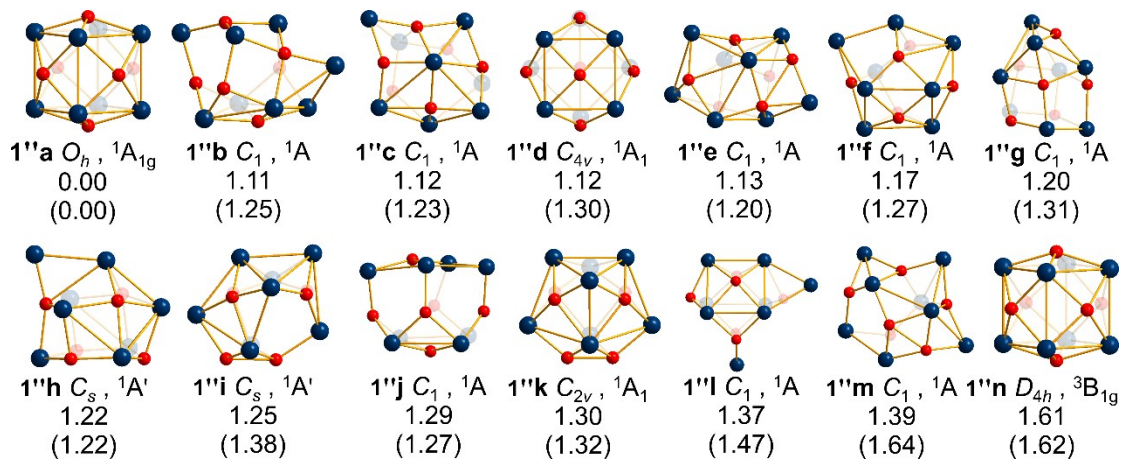


Figure S4. Low-lying isomers of monoanion $\text{Ni}_8\text{B}_6^{-1}$ with its relative energies indicated in eV at PBE0 and TPSSh (parentheses) levels, respectively.

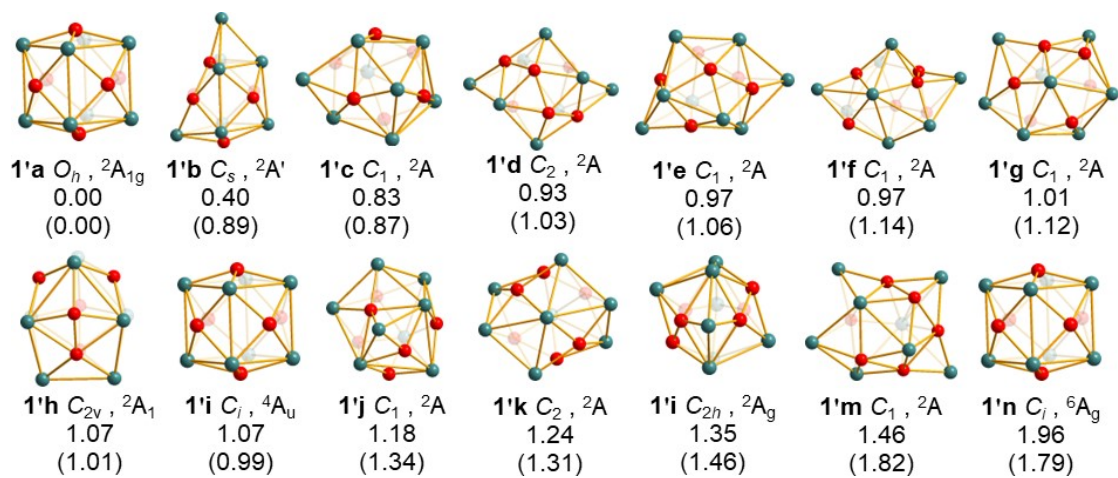


Figure S5. BOMD simulations of (a) O_h Ni_8B_6 (1), (b) O_h Pd_8B_6 (2), and (c) O_h Pt_8B_6 (3) at different temperatures with the RMSD and MAXD indicated in Å.

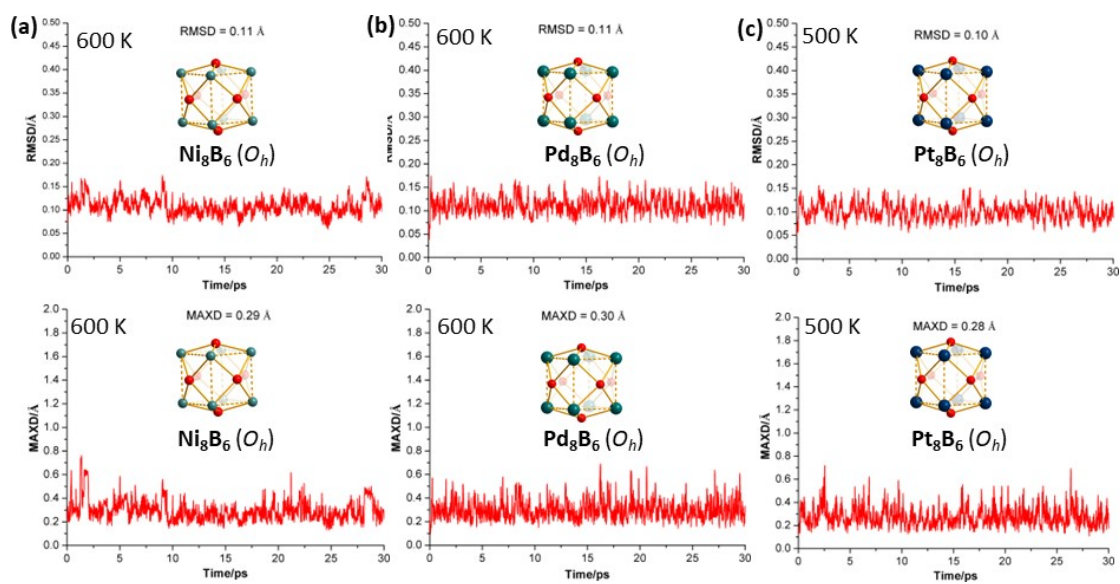


Figure S6 (a) The $1S^21P^61D^{10}$ 18-electron configurations of O_h Pd_8B_6 (**2**) and O_h Pt_8B_6 (**3**). The black and red solid lines refer to occupied and unoccupied orbitals, respectively. (b) AdNDP bonding patterns of O_h Pd_8B_6 (**2**) and O_h Pt_8B_6 (**3**) with the occupation numbers (ONs) indicated.

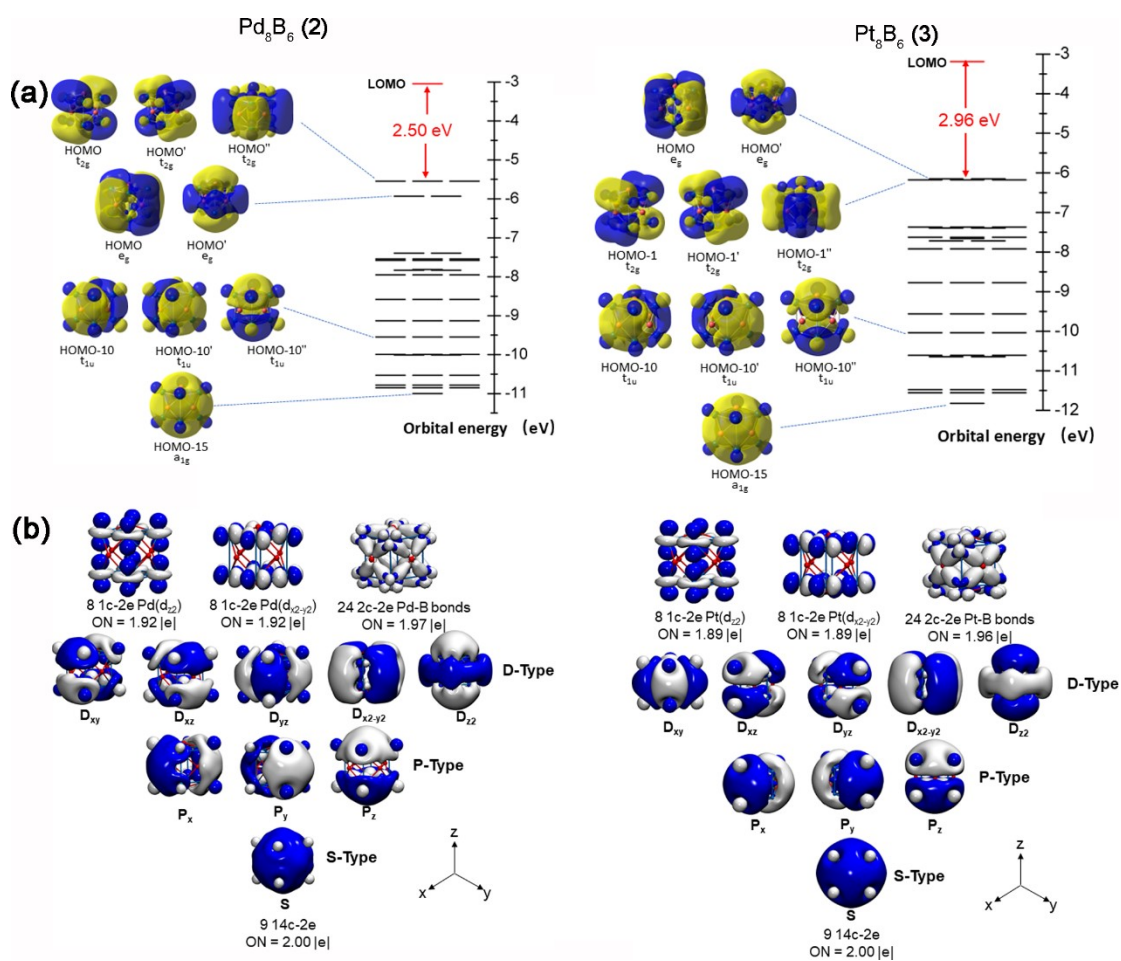


Figure S7. Simulated IR, Raman and UV-vis spectra of (a) O_h Pd₈B₆ and (b) O_h Pt₈B₆ at PBE0/6-311+G(d) level.

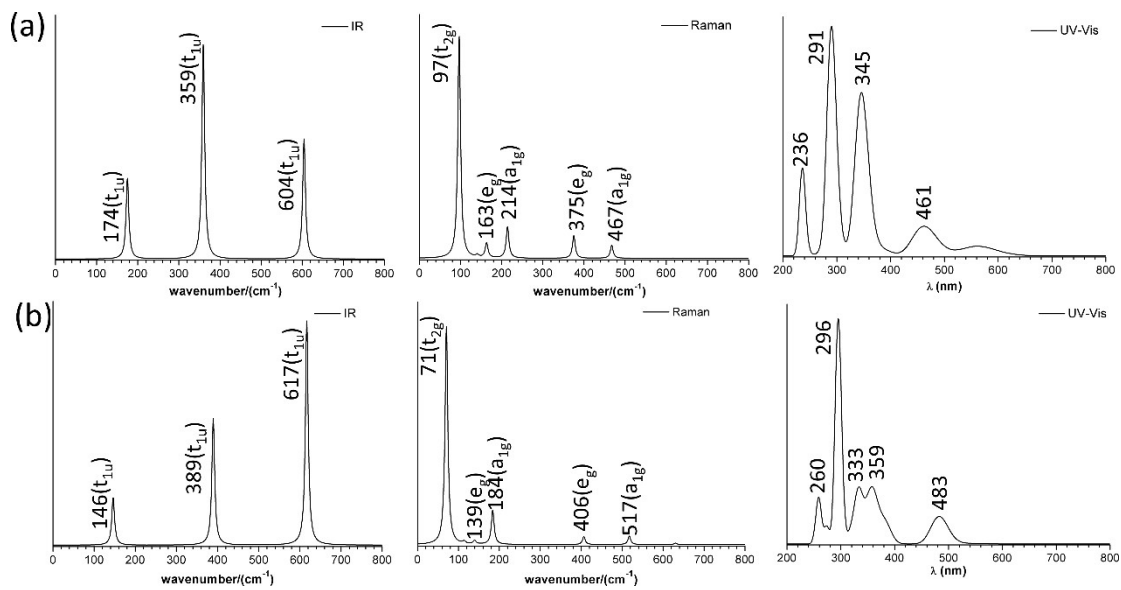


Table S1. Optimized cartesian coordinates (x, y, z) of (a) O_h Ni₆B₆ (**1**), (b) O_h Pd₆B₆ (**1'**), (c) O_h Pt₆B₆ (**1''**), and (d) O_h Ni₈B₆⁻¹ (**2**) at PBE0/6-311+G(d) level.

(a) O_h Ni₆ B₆ (**1**)

B	0.00000000	0.00000000	1.79487300
B	0.00000000	1.79487300	0.00000000
B	0.00000000	0.00000000	-1.79487300
B	0.00000000	-1.79487300	0.00000000
B	1.79487300	0.00000000	0.00000000
B	-1.79487300	0.00000000	0.00000000
Ni	-1.30575600	1.30575600	1.30575600
Ni	1.30575600	1.30575600	1.30575600
Ni	1.30575600	1.30575600	-1.30575600
Ni	-1.30575600	1.30575600	-1.30575600
Ni	-1.30575600	-1.30575600	-1.30575600
Ni	-1.30575600	-1.30575600	1.30575600
Ni	1.30575600	-1.30575600	-1.30575600
Ni	1.30575600	-1.30575600	1.30575600

(b) O_h Pd₆B₆ (**2**)

B	0.00000000	0.00000000	1.97396900
B	0.00000000	1.97396900	0.00000000
B	0.00000000	0.00000000	-1.97396900
B	0.00000000	-1.97396900	0.00000000
B	1.97396900	0.00000000	0.00000000
B	-1.97396900	0.00000000	0.00000000
Pd	-1.40539300	1.40539300	1.40539300
Pd	1.40539300	1.40539300	1.40539300
Pd	-1.40539300	-1.40539300	1.40539300
Pd	1.40539300	-1.40539300	-1.40539300
Pd	-1.40539300	-1.40539300	-1.40539300
Pd	-1.40539300	1.40539300	-1.40539300
Pd	1.40539300	1.40539300	-1.40539300
Pd	1.40539300	-1.40539300	1.40539300

(c) O_h Pt₆B₆ (**3**)

Pt	1.40832700	-1.40832700	-1.40832700
Pt	1.40832700	-1.40832700	1.40832700
Pt	1.40832700	1.40832700	1.40832700
Pt	1.40832700	1.40832700	-1.40832700
Pt	-1.40832700	-1.40832700	-1.40832700
Pt	-1.40832700	-1.40832700	1.40832700
Pt	-1.40832700	1.40832700	1.40832700
Pt	-1.40832700	1.40832700	-1.40832700
B	0.00000000	0.00000000	2.00454300
B	0.00000000	2.00454300	0.00000000
B	0.00000000	0.00000000	-2.00454300
B	0.00000000	-2.00454300	0.00000000
B	2.00454300	0.00000000	0.00000000
B	-2.00454300	0.00000000	0.00000000

(d) O_h Ni₈B₆⁻¹ (**1'**)

B	0.00000000	0.00000000	1.79487300
B	0.00000000	1.79487300	0.00000000

B	0.00000000	0.00000000	-1.79487300
B	0.00000000	-1.79487300	0.00000000
B	1.79487300	0.00000000	0.00000000
B	-1.79487300	0.00000000	0.00000000
Ni	-1.30575600	1.30575600	1.30575600
Ni	1.30575600	1.30575600	1.30575600
Ni	1.30575600	1.30575600	-1.30575600
Ni	-1.30575600	1.30575600	-1.30575600
Ni	-1.30575600	-1.30575600	-1.30575600
Ni	-1.30575600	-1.30575600	1.30575600
Ni	1.30575600	-1.30575600	-1.30575600
Ni	1.30575600	-1.30575600	1.30575600